

Highly stable polarization independent Mach-Zehnder interferometer

Michal Mičuda,^{1, a)} Ester Doláková,¹ Ivo Straka,¹ Martina Miková,¹ Miloslav Dušek,¹ Jaromír Fiurášek,¹ and Miroslav Ježek^{1, b)}

Department of Optics, Faculty of Science, Palacký University, 17. listopadu 1192/12, 77146 Olomouc, Czech Republic

We experimentally demonstrate optical Mach-Zehnder interferometer utilizing displaced Sagnac configuration to enhance its phase stability. The interferometer with footprint of 27×40 cm offers individually accessible paths and shows phase deviation less than 0.4 deg during a 250 s long measurement. The phase drift, evaluated by means of Allan deviation, stays below 3 deg or 7 nm for 1.5 hours without any active stabilization. The polarization insensitive design is verified by measuring interference visibility as a function of input polarization. For both interferometer's output ports and all tested polarization states the visibility stays above 93%. The discrepancy in visibility for horizontal and vertical polarization about 3.5% is caused mainly by undesired polarization dependence of splitting ratio of the beam splitter used. The presented interferometer device is suitable for quantum-information and other sensitive applications where active stabilization is complicated and common-mode interferometer is not an option as both the interferometer arms have to be accessible individually.

Mach-Zehnder interferometer¹ is an essential tool for many applications as well as in fundamental research². For instance, it can be used for an indirect measurement of any physical quantity that can be coupled to relative phase of the two interfering optical signals. This often requires the interferometer's arms to be individually accessible, while the interference contrast and phase stability represent further necessities. For telecom devices^{3,4} and sensors⁵ we often prefer integrated optical circuit implementation where interference contrast and phase stability are guaranteed by mode coupling between waveguides and inherently monolithic design, respectively. Free-space bulk-element interferometers, on the other hand, are highly configurable devices but far less stable compared to the integrated ones.

Various techniques have been adopted to stabilize the relative phase in Mach-Zehnder interferometric scheme. Thorough isolation against environmental noise could be quite efficient in lowering the phase uncertainty but requires a device optically contacted on ultra-low expansion material held in vacuum⁶. Though giving unbeatable phase stability, such a design limits working space and flexibility of the interferometer. Various methods of an active phase lock can be used instead to keep the phase locked to a particular setpoint employing a feedback loop, which has to be faster than the typical phase drift. Unfortunately, the overall noise of the feedback loop used ultimately limits the minimum attainable phase uncertainty to a few degrees^{7,8}. For low-level light applications, which typically employ single photon detectors with discrete output, the response of the feedback loop is superimposed with Poissonian photodetection noise⁹. To solve this issue, a strong probe signal can be used to sample the phase drift and recover the setpoint. During this stabilization stage, the single photon detectors have to be

gated off or otherwise isolated from the probe signal^{10,11}. Alternatively, a faint probe signal can be used, the optical power of which is acceptable for single photon detectors, at the expense of increasing the stabilization stage duration. Such single-photon level phase-stabilization loop is typically slower than 0.1 s^{9,12–15}.

Instead of resorting to an active approach, we can exploit intrinsic stability of some interferometric configurations. Sagnac interferometer¹⁶, for example, is well known for its inherently stable operation. This common-mode interferometer uses the same optical path for both interfering fields and hence the interferometer phase is automatically stabilized. Unfortunately, there is a big disadvantage—one cannot address individual interferometer's arm separately. An elegant solution is to displace the arms to obtain Mach-Zehnder interferometer where both arms can be accessed individually while maintaining Sagnac interferometer's phase stability to a great extent¹⁷.

In many interferometric applications the polarization state of the optical signal should be under control and the interferometer properties have to be independent of it. Important examples include optical quantum information protocols exploiting path as well as polarization degree of freedom of single photons^{18–22} and Faraday interaction characterization²³. Therefore, the interferometer's action should be verified to be polarization independent for such applications.

In this paper we describe the implementation of Mach-Zehnder interferometer using displaced Sagnac configuration (MZDS) and verify its basic properties, particularly interference visibility, polarization sensitivity, and phase stability.

The experimental setup is shown in the Fig. 1. The preparation stage consists of filtered laser source with reference detector and linear polarization preparation. Laser diode (OZ optics, FOSS-01-3S-5/125-810-S-1) with central wavelength of 816 nm and full spectral width at half maximum (FWHM) of 4 nm is spectrally filtered by narrow interference filter (Andover Corporation) cen-

^{a)}micuda@optics.upol.cz

^{b)}jezek@optics.upol.cz

tered at 814 nm with FWHM of 2 nm to match the design wavelength of optical components employed. Estimated coherence length after the filter reads 0.150 mm. Optical signal is further coupled in single-mode optical fiber (Nufern HP780) and split by a 3 dB fiber coupler (FC) from Sifam. One part of the signal goes to a photodiode (D0), which serves as a reference detector of the source optical power. The rest of the laser light passes the polarizing beam splitter (PBS) with extinction ratio larger than 1000:1 and the half wave plate (HWP) to set a proper polarization state. Both components are supplied by Eksma Optics.

The MZDS interferometer itself consists of a 1" beam splitter cube (BS) from Optida with antireflection coated sides, three 1" dielectric mirrors (Thorlabs BB1-E03), and two antireflection coated 1 mm thick glass plates (GP). The interferometer arms are 1.34 m long and displaced by 8 mm. The distance between beams was chosen as a reasonable trade-off between available clear aperture of the components and convenient individual addressing of the beams. The manufacturer of the beam splitter cube specifies splitting ratio of 50 : 50 for both polarization modes. Our measurement shows the splitting ratio of 45 : 55 for the horizontal polarization state (P polarization) and 43 : 57 for the vertical polarization state (S polarization). The reflectance of the mirrors employed reveals only negligible dependence on the input polarization state. However, small phase shift is induced between S and P polarization modes, which does not influence the interferometer performance as both arms feel the same phase shift. If distortion-free propagation of the polar-

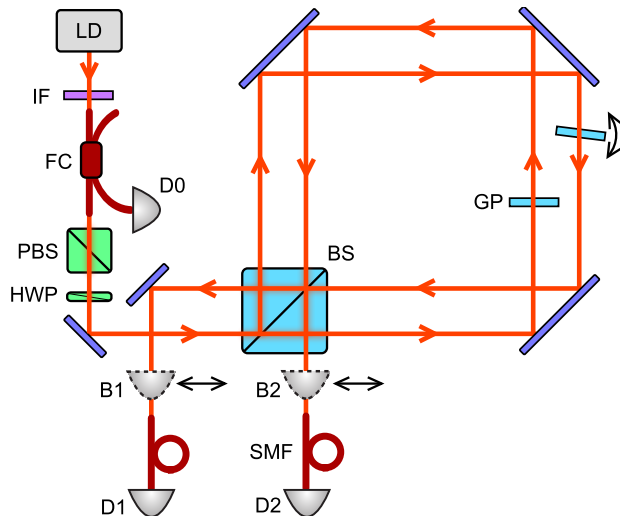


FIG. 1. (Color online) Experimental realization of Mach-Zehnder interferometer using displaced Sagnac geometry. Polarized laser light is injected to the setup, split and superimposed again by the single beam splitter cube (BS), and detected at the output either by bulk photodiodes B1 and B2 or by single-mode-fiber coupled photodiodes D1 and D2 to provide a definition of the spatial mode. See text for more details.

ization state within the interferometer is required, low-dephasing dielectric mirrors should be employed, for example OA019 from Femto-Optics. We have measured the phase induced between S and P modes by this mirror to be smaller than 1 deg. Because of displaced Sagnac configuration, it is not convenient to scan interference fringes using piezo-crystal mounted mirror. All three mirrors are kept fixed after the initial alignment and the relative optical phase of the interferometer is set by tilting one of the glass plates. Mirrors and glass plates are mounted using Newport Suprema SN100C Series mirror mounts and connected to Newport RS-4000 optical table by 1" diameter 65 mm high brass pedestals. The beam splitter cube is epoxy glued directly to the pedestal.

The beams at interferometer's output ports are optimally coupled into single mode optical fibers to provide a definition of the spatial mode. These fibers are then guided to detectors. The output optical intensity is measured by silicon p-i-n photodiodes D1 and D2 (Thorlabs DET36A). Alternatively, fiber-coupled photon counters can be connected easily when the interferometer is operated at single photon level. The fringe visibility²⁴ is calculated using Michelson's formula

$$V = \frac{I_{\max} - I_{\min}}{I_{\max} + I_{\min}}, \quad (1)$$

where I_{\max} and I_{\min} are the maximum and the minimum optical intensities at the particular output port, respectively. We measured the interferometric visibility for various angles of HWP in the preparation stage, which corresponds to different polarization states ranging from P to S polarizations. The visibility dependence on the input polarization state is shown in the Fig. 2. We developed a theoretical model of the visibility based on actual parameters of the beam splitter cube. The measured and theoretically predicted values of the visibility at D1 and D2 for horizontal and vertical polarization states are summarized in the Table I. According to the theory we expect the unity visibility in the first output port for all polarization states which is in excellent agreement with measured data—the visibility higher than 99.8% was reached in this port for all tested polarization states. In the second output port, we observed approximately 0.7% difference between theory and experiment for horizontal polarization state and 2.5% for vertical polarization state. The H/V discrepancy is probably caused by a variation of the splitting ratio of the beam splitter cube and the reflectance of the mirrors over the active area of these components.

port	theoretical visibility [%]		measured visibility [%]	
	H	V	H	V
D1	100	100	99.96 ± 0.01	99.98 ± 0.01
D2	98.02	96.16	97.33 ± 0.03	93.60 ± 0.09

TABLE I. The theoretically estimated and the measured values of the interferometric visibility at D1 and D2 outputs for horizontally and vertically polarized light.

For the sake of comparison, the output intensity was acquired also by bulk photodiodes placed directly after the MZDS interferometer. The measured values of the visibility at output ports B1 and B2 are summarized in the Table II. It shows that single mode selection increases spatial mode matching and thus the visibility for all polarization states in both output ports by approximately 2%.

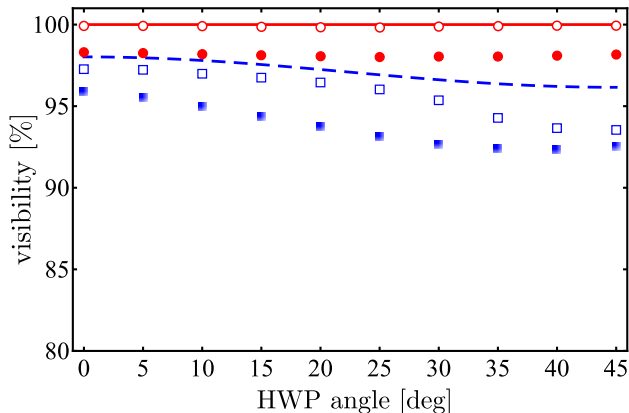


FIG. 2. (Color online) The visibility dependence on the input linear polarization state: 0 deg and 45 deg correspond to horizontal (P polarization) and vertical polarization state (S polarization), respectively. Curves stand for the theoretical values of visibility: The first output port is depicted by red color (solid), the second one by blue color (dashed). \circ represents measured visibility at D1, \square represents measured visibility at D2, \bullet represents measured visibility at B1, and \blacksquare represents measured visibility at B2. Statistical errors are smaller than the symbol size.

The visibility measurement repeated on daily basis shows only negligible variation proving its long-term stability despite of ambient temperature fluctuations. Interferometer phase stability is another crucial parameter which is affected by air fluctuations, mechanical vibrations and temperature changes. To demonstrate the phase stability of the MZDS interferometer we acquired the intensity at detector D1 every second for ten hours. The input polarization state was set to the horizontal linear polarization and the initial phase was set to 0 deg, thus having interference minimum at the output port D1. The intensity at the reference detector D0 has been measured simultaneously. Both the photocurrents have been recorded by 12 bit data acquisition system (Pico Technol-

port	measured visibility [%]	
	H	V
B1	98.35 ± 0.03	98.2 ± 0.1
B2	95.93 ± 0.05	92.61 ± 0.04

TABLE II. The experimentally observed values of the interferometric visibility at B1 and B2 outputs for horizontally and vertically polarized light, measured by bulk photodetectors.

ogy PicoLog 1216) for 10 hours. During the measurement period the temperature has been stable within 1 K. The interferometric phase is calculated from the measured intensity at D1 corrected for the power fluctuation of the laser source. We employ the Allan variance²⁵ to evaluate the optimum duration of the measurement—the integration time of the single acquisition that yields the lowest possible phase uncertainty, which corresponds to the minimum Allan deviation. Further, the maximum duration of the measurement is estimated to keep the phase uncertainty reasonably small. The Allan deviation corresponding to the integration time τ reads

$$\sigma(\tau) = \sqrt{\frac{1}{2N} \sum_{n=1}^{N-1} (\bar{y}_{n+1} - \bar{y}_n)^2}, \quad (2)$$

where the overall time T of the long-term phase stability measurement is divided into N intervals, $T = N\tau$, and the average phase value \bar{y}_n is computed in each interval.

Typical results of the phase stability of the MZDS interferometer are shown in Fig. 3. The minimum Allan deviation less than 0.39 deg is demonstrated for the integration time of about 250 s with no stabilization technique employed. This phase uncertainty corresponds to the interferometer arm length deviation of 0.87 nm and the relative length deviation of 0.65×10^{-9} . If we allow ourselves to have the phase deviation less than 3 deg then the duration of the measurement can be extended up to 1.5 hours. The measured phase uncertainty of the MZDS interferometer can be compared with phase stability of Mach-Zehnder interferometer for heterodyne metrology presented by Niwa and collaborators⁶. They were able to keep the interferometer arm length deviation below 20 pm over a hour. This excellent stability figure was achieved by building their interferometer on ultra-low expansion glass base plate with dimensions of 5×5 cm and placing the whole setup into a vacuum chamber with temperature stabilization within 1 mK over four hours. The resulting relative length deviation of about $0.2 \cdot 10^{-9}$ per hour is better by a factor of ten than what we have shown here for the MZDS interferometer operating under much less demanding conditions. Further, the observed passive phase stability is comparable with an active phase lock loop, the noise of which can easily induce the overall phase uncertainty of an order of 1 deg even if measured at high frequency where the ambient noise is significantly lower. Takeno et al⁸ showed the actively locked phase uncertainty of 1.5 deg at 1 MHz sideband with the bandwidth of 30 kHz. Eberle et al.²⁶ demonstrated a sub-degree phase uncertainty at 8 MHz sideband with the bandwidth of 200 kHz for up to 15 minutes. Phase noise suppression at acoustic and lower frequencies and for longer times is typically not crucial for quantum continuous-variables experiments with sideband encoded information but it is generally very important for single photon level interferometric measurements with prolonged data acquisition times¹⁷.

In conclusion, we have reported the inherently sta-

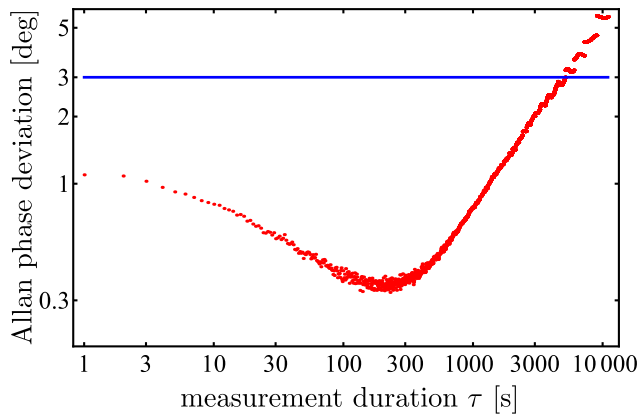


FIG. 3. (Color online) Phase stability of the Mach-Zehnder interferometer using displaced Sagnac configuration. Red dots denote measured Allan phase deviation as a function of integration time. Blue solid line represents 3 deg deviation level. See the text for details.

ble Mach-Zehnder interferometer in displaced Sagnac geometry, examined its visibility, polarization sensitivity and phase stability. The visibility of the interferometer slightly depends on the polarization state. We have measured approximately 3.5% difference in visibility between the S and P polarization modes at one output port of the interferometer and virtually no difference at the other one. This behavior agrees reasonably with the simple theoretical model developed, which takes into account measured splitting ratios of the beam splitter cube for both the polarization modes. With more balanced beam splitter the overall performance of the interferometer will improve as can be already seen at its first port where the visibility does not depend on the splitting ratio and is given solely by mode matching. At this port we consistently observe the interference visibility higher than 99.8% with negligible dependence on the input polarization. Further, we have explored long-term stability of the interferometric phase. We have demonstrated the root-mean-square phase noise of the MZDS interferometer as low as 0.39 deg within the measurement time of 250 s and of about 3 deg when integrated from 0.2 mHz to 1 Hz. We expect no significant phase noise for higher frequencies because of the closeness of MZDS interferometer's paths and thus its virtual immunity to acoustic waves with frequencies up to tens kHz. The inherent robustness and notable long-term passive phase stability make the MZDS interferometer good candidate to encode a spatial quantum bit carried by a single photon in various quantum information protocols. Together with low polarization sensitivity and ease to address its individual arms, it enables the hyper-encoding using both the spatial and polarization degrees of freedom. Alternatively, Jamin-Lebedeff interferometer²⁷ formed by a pair of calcite prisms can be used for applications where the polarization insensitivity is not required²⁸. The presented interferometer device thus seems suitable for quantum-information and other sensitive applications where active

phase stabilization is complicated and common-mode interferometer is not an option as both interfering arms have to be accessible individually.

ACKNOWLEDGMENTS

This work was supported by the Czech Science Foundation (GACR 13-20319S) and by the Palacký University (IGA-PrF-2014008).

- ¹L. Zehnder, *Z. Instrumentenk* **11**, 275 (1891), L. Mach, *Z. Instrumentenk* **12**, 89 (1892).
- ²M. Suda, C. Pacher, M. Peev, M. Dušek, and F. Hipp, *Quant. Inf. Processing* **12**, 1915 (2013).
- ³Ed. W.S.C. Chang, *RF Photonic Technology in Optical Fiber Links* (Cambridge University Press, 2002).
- ⁴Eds. A. Chen and E. Murphy, *Broadband Optical Modulators: Science, Technology, and Applications* (CRC Press, 2011).
- ⁵A.L. Washburn and R.C. Bailey, *Analyst* **136**, 227 (2011).
- ⁶Y. Niwa, K. Arai, A. Ueda, M. Sakagami, N. Gouda, Y. Kobayashi, Y. Yamada, and T. Yano, *App. Opt.* **48**, 6105 (2009).
- ⁷S. Suzuki, H. Yonezawa, F. Kannari, M. Sasaki, and A. Furusawa, *Appl. Phys. Lett.* **89**, 061116 (2006).
- ⁸Y. Takeno, M. Yukawa, H. Yonezawa, and A. Furusawa, *Opt. Express* **15**, 4321 (2007).
- ⁹D. Pulford, C. Robillard and E. Huntington, *Rev. Sci. Instrum.* **76**, 063114 (2005).
- ¹⁰G.B. Xavier and J.P. von der Weid, *Opt. Lett.* **36**, 1764 (2011).
- ¹¹A. Cuevas, G. Carvacho, G. Saavedra, J. Carine, W.A.T. Nogueira, M. Figueroa, A. Cabello, P. Mataloni, G. Lima, and G.B. Xavier, *Nat. Commun.* **4**, 2871 (2013).
- ¹²V. Makarov, A. Brylevski, and D.R. Hjelm, *Appl. Opt.* **43** 4385 (2004).
- ¹³L. Bartušková, A. Černoch, R. Filip, J. Fiurášek, J. Soubusta, and M. Dušek, *Phys. Rev. A* **74**, 022325 (2006).
- ¹⁴L. Bartušková, M. Dušek, A. Černoch, J. Soubusta, and J. Fiurášek, *Phys. Rev. Lett.* **99**, 120505 (2007).
- ¹⁵M. Míková, H. Fikerová, I. Straka, M. Míčuda, J. Fiurášek, M. Ježek, and M. Dušek, *Phys. Rev. A* **85**, 012305 (2012).
- ¹⁶G. Sagnac, *Comptes Rendus* **157**, 1410 (1913).
- ¹⁷T. Nagata, R. Okamoto, J.L. O'Brien, K. Sasaki, and S. Takeuchi, *Science* **316**, 726 (2007).
- ¹⁸M.P. Almeida, F. de Melo, M. Hor-Meyll, A. Salles, S. P. Walborn, P.H. Souto Ribeiro, L. Davidovich, *Science* **316**, 579 (2007).
- ¹⁹X.-Y. Xu, J.-S. Xu, C.-F. Li, Y. Zou, and G.-C. Guo, *Phys. Rev. A* **83**, 010101(R) (2011).
- ²⁰R. Okamoto, J.L. O'Brien, H.F. Hofmann, T. Nagata, K. Sasaki, S. Takeuchi, *Science* **323**, 483 (2009).
- ²¹Ryo Okamoto, Jeremy L. O'Brien, Holger F. Hofmann, and Shigeki Takeuchi, *Proc. Natl. Acad. Sci. U.S.A.* **108**, 10067 (2011)
- ²²X.-Q. Zhou, T.C. Ralph, P. Kalasuwan, M. Zhang, A. Peruzzo, B.P. Lanyon, and J.L. O'Brien, *Nat. Commun.* **2**, 413 (2011).
- ²³J.M. LaForge and G.M. Steeves, *Appl. Phys. Lett.* **91**, 121115 (2007)
- ²⁴M. Born and E. Wolf, *Principles of optics* (Cambridge University Press, 1997).
- ²⁵D.W. Allan, *Proceedings of the IEEE* **54**, 221 (1966).
- ²⁶T. Eberle, V. Händchen, and R. Schnabel, *Opt. Express* **21**, 11546 (2013).
- ²⁷J.C. Jamin, *Annalen der Physik und Chemie* **174** 345 (1856); A.A. Lebedeff, *Rev. Opt.* **9**, 385 (1930); M. Francon, *Appl. Opt.* **3**, 1033 (1964).
- ²⁸J.L. O'Brien, G.J. Pryde, A.G. White, T.C. Ralph, and D. Branning, *Nature* **426**, 264 (2003).